Article

Not peer-reviewed version

Lipid perturbations in the saliva, plasma, and feces of patients with non-small cell lung cancer

Bo Young Hwang , Jae Won Seo , Can Muftuoglu , Ufuk Mert , Filiz Guldaval , Milad Asadi , Haydar Soydaner Karakus , Tuncay Goskel , Ali Veral , Ayse Caner * , Myeong Hee Moon *

Posted Date: 7 August 2023

doi: 10.20944/preprints202308.0522.v1

Keywords: lung cancer, NSCLC, lipidomic analysis, saliva, plasma, feces, LC-ESI-MS/MS

Article

Lipid Perturbations in the Saliva, Plasma, and Feces of Patients with Non-Small Cell Lung Cancer

Bo Young Hwang [1], Jae Won Seo [1], Can Muftuoglu [2,3], Ufuk Mert [3,4], Filiz Guldaval [5], Milad Asadi [2,3], Haydar Soydaner Karakus [6], Tuncay Goksel [3,6], Ali Veral [7], Ayse Caner [2,3,8,*] and Myeong Hee Moon [1,*]

[1] Department of Chemistry, Yonsei University, Seodaemun-gu, Seoul, 03722, Korea
[2] Institute of Health Sciences, Department of Basic Oncology, Ege University, Izmir, Turkey
[3] Translational Pulmonary Research Center, Ege University (EgeSAM), Izmir, Turkey
[4] Ataturk Health Care Vocational School, Ege University, Izmir, Turkey
[5] Chest Disease Department, Izmir Dr. Suat Seren Chest Disease and Surgery Training and Research Hospital, Izmir, Turkey
[6] Department of Pulmonary Medicine, Faculty of Medicine, Ege University, Izmir, Turkey
[7] Department of Pathology, Faculty of Medicine, Ege University, Izmir, Turkey
[8] Department of Parasitology, Faculty of Medicine, Ege University, Izmir, Turkey
* Correspondence: mhmoon@yonsei.ac.kr; Tel.: 82-2-2123-5634 (M.H.M), ayse.caner@ege.edu.tr; Tel.: +90-505-485-5994 (A.C)

Abstract: A comprehensive lipid profile was analyzed in patients with non-small cell lung cancer (NSCLC) using nanoflow ultrahigh-performance liquid chromatography-electrospray ionization-tandem mass spectrometry. The study investigated 297, 202, and 166 lipids in saliva, plasma, and fecal samples, respectively, comparing NSCLC patients to healthy controls. Lipids with significant changes (>2-fold, $p<0.05$) were further analyzed in each sample type. Both saliva and plasma exhibited similar lipid alteration patterns in NSCLC, but saliva showed more pronounced changes and fecal lipids had weak correlation with those of saliva and plasma. Total triglycerides (TGs) increased (>2–3 folds) in plasma and saliva but decreased in fecal samples. Three specific TGs (50:2, 52:5, and 54:6) were significantly increased in NSCLC across all sample types. A common ceramide species (d18:1/24:0) decreased in both plasma and saliva but increased in fecal samples. Additionally, phosphatidylinositol 38:4 decreased by approximately 2-fold in plasma and saliva. Phosphatidylserine 36:1 was selectively detected in saliva and showed a subsequent decrease, making it a potential biomarker for predicting lung cancer. The study identifies 27 salivary, 10 plasma, and 16 fecal lipids as candidate markers for NSCLC by statistical evaluations. Moreover, it highlights the potential of saliva in understanding changes in lipid metabolism associated with NSCLC.

Keywords: lung cancer; NSCLC; lipidomic analysis; saliva; plasma; feces; LC-ESI-MS/MS

1. Introduction

Lung cancer (LC) is the second most diagnosed cancer worldwide, with high incidence and mortality rates (2.2 million new cases and 1.8 million deaths in 2020) [1,2]. Despite advancements in lung cancer diagnosis and treatment, high mortality and poor prognosis persist because of a lack of reliable early detection, leading to challenges in performing curative surgical procedures [3]. Lung cancer is categorized into two main types, small cell lung cancer (SCLC) and non-small cell lung cancer (NSCLC), with the latter comprising approximately 85% of cases. Lipids are the major constituents of biological membranes in tissues and are present in various body fluids, such as serum, urine, saliva, and tears. They play crucial physiological and pathological roles, including signal transduction between cells, cell proliferation and death, and energy storage. Recent advancements in high-performance liquid chromatography-electrospray ionization-tandem mass spectrometry (HPLC-ESI-MS/MS) have facilitated more accurate and convenient analysis of lipid profiles [4,5]. Lipid perturbations have been associated with metabolic changes in several diseases including diabetes, various cancers, and cardiovascular diseases, making them potential biomarkers for disease

 doi:10.20944/preprints202308.0522.v1

diagnosis and prognosis [6-9]. Notably, substantial changes in the phospholipid profiles of NSCLC tissues [4,10] such as a reduction in unsaturated fatty acids, an increase in saturated fatty acids and lysophosphatidylethanolamine (LPE) in NSCLC serum [11], and a substantial decrease in phosphatidylethanolamine (PE) in the plasma of patients with lung cancer [9] have been reported. While most lipidomic analyses of lung cancer have focused on tissues and blood samples, it would be highly beneficial to detect lung cancer at an early stage using molecular biomarkers derived from easily accessible and non-invasive clinical samples.

Saliva is a clinically informative body fluid that serves important functions in protecting oral tissues, regulating oral conditions and pH, and initiating food digestion [12,13]. Saliva contains electrolytes, enzymes, proteins, carbohydrates, metabolites, nucleic acids, lipids, mucins, and other substances, many of which are transferred from blood. Saliva can be used to identify biomarkers for disease diagnosis and monitoring [14-17]. As a potential diagnostic fluid, saliva collection is easy and non-invasive and patient compliance is high. However, investigations of salivary lipids associated with diseases are limited. A recent study focused on optimizing saliva volumes for lipidomic analysis using nanoflow ultrahigh performance liquid chromatography-tandem mass spectrometry (nUHPLC-MS/MS) [18].

Feces are also easily collected, and contain various components such as bacteria, intestinal epithelial cells, undigested food-derived fiber, proteins, DNA, lipids, and metabolites, which reflect the final outcome of nutrient intake, digestion, and absorption by intestinal bacteria and the gastrointestinal tract [19]. Although fecal metabolites have been extensively studied in various health conditions, including obesity, cardiovascular disease, and inflammatory bowel disease [20-22], lipidomic analysis of fecal samples is relatively rare, with only a few studies focusing on the methodological evaluation of lipidomic profiling [23-25]. Recent studies have revealed lipidomic alterations in human fecal samples related to diseases such as metabolic syndrome [26] and progressive liver disease [27].

Despite the potential for analyzing lipids in non-invasive samples such as saliva and feces, most lipidomic analyses in lung cancer have primarily focused on plasma or tissues [9,11,28-30], and systematic approaches to studying fecal and salivary lipid profiles in patients with lung cancer are lacking. In this study, we conducted comprehensive lipidomic profiling of saliva, plasma, and fecal samples from patients diagnosed with NSCLC using nUHPLC-MS/MS to identify candidate biomarkers. Tandem MS analysis allowed the identification of the molecular structures of 634 lipids in saliva, 408 in plasma, and 206 in fecal samples. Selected lipids were quantified by targeted quantification using selective reaction monitoring. Statistical evaluation was performed to identify the lipid species that showed significant alterations in the saliva, plasma, and fecal samples of patients with lung cancer, which were subsequently screened and evaluated as candidate biomarkers.

2. Materials and Methods

2.1. Materials and reagents

A total of 48 lipid standards were used in this study and are listed in Supplementary Table S1. All lipid standards were purchased from Polar Lipids Inc. (Alabaster, AL, USA). Nonendogenous lipids with odd-numbered or deuterated acyl chains were used for calibration. An internal standard lipid mixture was prepared by combining 19 lipid standards (lysophosphatidylcholine (LPC) 18:1-D_7, phosphatidylcholine (PC) 15:0/18:1-D_7, lysophosphatidylethanolamine (LPE) 18:1-D_7, phosphatidylethanolamine (PE) 15:0/18:1-D_7, lysophosphatidic acid (LPA) 17:1, phosphatidic acid (PA) 15:0/18:1-D_7, lysophosphatidylglycerol (LPG) 13:0, phosphatodylglycerol (PG) 15:0/18:1-D_7, lysophosphatidylinositol (LPI) 13:0, phosphatidylinositol (PI) 15:0/18:1-D_7, lysophosphatidylserine (LPS) 13:0, phosphatidylserine (PS) 15:0/18:1-D_7, sphingomyelin (SM) d18:1-D_9/18:1, ceramide (Cer) d18:1-D_7/24:0, hexosylceramide (HexCer) d18:1-D_7/15:0, and Hex2Cer d18:1-D_7/15:0, diacylglycerol (DG) 15:0_18:1-D_7, triglycerides (TG) 15:0_18:1-D_7_15:0, cholesteryl ester (CE) 18:1-D_7) from Avanti Polar Lipids, Inc. Calibration and internal lipid standards were added to the samples prior to lipid extraction for validation. HPLC-grade solvents, including water, acetonitrile, methanol, isopropyl

 doi:10.20944/preprints202308.0522.v1

alcohol (IPA), and methyl-tert-butyl ether (MTBE), were purchased from Avantor Performance Materials (Center Valley, PA, USA). Ammonium formate and ammonium hydroxide were obtained from Sigma-Aldrich (St. Louis, MO, USA). Silica capillary tubes with an inner diameter of 100 μm and an outer diameter of 360 μm were purchased from Polymicro Technology, LLC (Phoenix, AZ, USA). Two types of packing materials were used to prepare a homemade capillary column: ODS-P C-18 particles (3 μm and 100 Å) from Isu Industry Corp. (Seoul, Korea) for a self-assembled frit and ethylene bridged hybrid (BEH) shield C18 particles (1.7 μm and 130 Å) from Waters (Milford, MA, USA) for the analytical column. The latter was obtained by unpacking an ACQUITY UPLC BEH Shield C18 column (2.1 mm × 100 mm) from Waters.

2.2. Human samples

Human samples were obtained from patients diagnosed with NSCLC (25 plasma and 26 saliva and fecal samples) and healthy adults as controls (30 plasma and 22 saliva and fecal samples) in the Chest Diseases, Faculty of Medicine, Ege University, and Suat Seren Chest Diseases and Surgery Education and Research Hospital, Izmir, Turkey. The demographic and clinical information of the patients was recorded. The pathological diagnosis of NSCLC was confirmed in 26 patients using either histological or cytological approaches. For the control group, 30 healthy individuals without cancer and family history of cancer were enrolled and matched with patients with cancer in terms of age, sex, and chronic diseases. Fecal and saliva samples were collected from patients diagnosed with NSCLC and healthy adults. For saliva samples, patients fasted for at least 8 h before sampling and underwent their last dental care the previous night. For fecal samples, patients discontinued the use of antacids, barium, anti-diarrhea medications, or oily laxatives for at least 72 h before sampling. Plasma samples were collected between 7 AM and 10 AM after an overnight fast of 8–12 hours. Collected samples were immediately aliquoted and stored at -80°C before being shipped to Prof. Moon's lab at Yonsei University using a medical express service under dry ice. Before shipping, saliva and fecal samples were mixed with an organic solvent mixture (1.0 mL of MTBE and 0.3 mL of CH_3OH per 500 μL of saliva or 150 mg of feces) and stored at −80°C to prevent lipid deterioration due to exposure to external temperature during shipment. The organic solvents used in this study were the same as those used for the lipid extraction.

2.3. Lipid extraction

Human samples (saliva, plasma, and feces) in the frozen state were thawed at room temperature and vortexed for 20 min. For lipid extraction, 500 μL of saliva and 100 μL of plasma were used for each sample, and the internal standard mixtures were added. The mixture was lyophilized in a Bondiro MCFD 8508 freeze-dryer vacuum centrifuge (IlShinBioBase, Yangju, Korea). The resulting dried powder samples were used for lipid extraction. For feces, each fecal sample was lyophilized and then suspended in water at a concentration of 60 μL/mg, following protocols from the literature [23,31]. Prior to extraction, the internal standard mixture was spiked to180 μL of the suspension (equivalent to 3 mg). Subsequently, each dried saliva and plasma sample or fecal suspension (180 μL) was dissolved in 0.3 mL of CH_3OH, cooled in an ice bath for 10 min, and mixed with 1.0 mL of MTBE. After vortexing the mixture for 1 h, 0.25 mL MS-grade H_2O was added, followed by vortexing for another 10 min and centrifugation at 1000 × g for 10 min. The supernatant was collected, and the aqueous layer was mixed with 0.3 mL MTBE to extract any remaining lipids. This mixture was subjected to 2 min of tip sonication and 10 min of centrifugation at 1000 × g. The resulting organic layer was combined with the previously collected organic solvent layer. The mixture of the two layers was dried using an Evatros Mini Evaporator (Goojung Engineering, Seoul, Korea) with nitrogen gas. The dried lipids were dissolved in 150 μL of MeOH: $CHCl_3$: H_2O (17: 1: 2 volume ratio) and stored at −80°C until nUHPLC-ESI-MS/MS analysis.

 doi:10.20944/preprints202308.0522.v1

2.4. Lipid analysis with nUHPLC-ESI-MS/MS

Lipid analysis by nUHPLC-ESI-MS/MS was conducted using two systems: an Ultimate 3000 RSLCnano System coupled with a Q Exactive mass spectrometer from Thermo Scientific (San Jose, CA, USA) for lipid identification, and a model nanoACQUITY UHPLC system from Waters (Milford, MA, USA) coupled with a TSQ Vantage triple quadrupole mass spectrometer for targeted quantification from Thermo Scientific. Analytical columns were prepared in the laboratory by packing 1.7 μm BEH Shield C18 particles into pulled-tip capillaries (approx. 8 cm long), following the same procedure as described in a previous report [18]. A binary gradient run was employed with two mobile phases, H_2O: CH_3CN (9: 1, v/v) for A and IPA: CH_3OH: CH_3CN: H_2O (7: 1.5: 1: 0.5, v/v/v/v) for B, both containing a mixture of ionization modifiers (0.5 mM NH_4HCO_2 and 5 mM NH_4OH). Approximately, 0.3 μL was injected in all the extracted lipid samples. The binary gradient elution was initiated by increasing the composition of B to 70% over 5 min, then to 100% over 20 min at a flow rate of 0.8 μL/min and was maintained at 100% for 30 min, then reduced to 0% B, and maintained for 5 min. The ESI voltages applied to the MS system were 3.0 kV and 1.5 kV for positive and negative ion modes, respectively, with an ion transfer tube temperature of 350°C. A full MS scan mode with data-dependent MS/MS analysis was used in both positive and negative ion modes to qualitatively analyse the lipid molecular structure. Lipids were identified using LipidMatch [32]. The identified lipid molecular structures were confirmed manually within a tolerance of 5 ppm of the precursor ion mass. Targeted lipid quantification was performed using selected reaction monitoring in polarity switching mode in a single nUHPLC run. The lipid classes detected in the positive ion cycle were LPC, PC, etherLPC, etherPC, LPE, PE, etherLPE, etherPE, SM, Cer, HexCer, Hex2Cer, DG, TG, and CE. The classes LPA, PA, LPS, PS, LPG, PG, LPI, and PI were detected in the negative ion mode. The precursor and quantifier ions for each lipid class for selected reaction monitoring quantification are listed in Table S2, along with the collision energy for the MS/MS analysis that varied across lipid classes. Quantification was performed using an Xcalibur (Thermo Scientific) based on the calibration curves established for each lipid class. Student's t-test was conducted using SPSS software (version 26, IBM Corp., Armonk, NY, USA), and principal component analysis (PCA) was performed using Minitab 17 (Minitab, Inc., State College, PA, USA).

2.5. Method validation

Calibration curves were established for different lipid classes in the three human samples (saliva, plasma, and feces), where each pooled saliva, plasma, and fecal sample was prepared by mixing a small portion of the individual samples (26 saliva, 25 plasma, and 26 feces from 26 patient samples). For each pooled sample, calibration standard solutions were prepared by varying the concentration of a mixture of 18 calibration standards (0.10, 0.20, 0.40, 0.60, 0.80, 1.00, 2.00, and 4.00 pmol/μL) as listed in Table S2 with a fixed concentration of the internal standard mixture. Calibration curves were constructed using the normalized peak area of each calibration standard relative to the peak area of the internal standard in five replicate runs of nUHPLC-ESI-MS. The slopes and intercepts of the calibration curves are presented in Table S3. The limit of detection (LOD) and limit of quantitation (LOQ) were based on signal-to-noise ratios (S/N) of 3 and 10, respectively (Table S4).The Materials and Methods should be described with sufficient details to allow others to replicate and build on the published results. Please note that the publication of your manuscript implicates that you must make all materials, data, computer code, and protocols associated with the publication available to readers. Please disclose at the submission stage any restrictions on the availability of materials or information. New methods and protocols should be described in detail while well-established methods can be briefly described and appropriately cited.

Research manuscripts reporting large datasets that are deposited in a publicly available database should specify where the data have been deposited and provide the relevant accession numbers. If the accession numbers have not yet been obtained at the time of submission, please state that they will be provided during review. They must be provided prior to publication.

Preprints (www.preprints.org) | NOT PEER-REVIEWED | Posted: 7 August 2023 doi:10.20944/preprints202308.0522.v1

Interventionary studies involving animals or humans, and other studies that require ethical approval, must list the authority that provided approval and the corresponding ethical approval code.

3. Results

3.1. Identification and target-based lipid quantification

The non-targeted identification of lipid species was performed using nUHPLC-ESI-MS/MS. Three pooled samples (consisting of control and lung cancer group samples for saliva, feces, and plasma) were analysed, and the base peak chromatograms of each sample are shown in Figure S1 of the Supplementary data. Through data-dependent collision-induced dissociation experiments and analysis of MS/MS spectra, 634, 408, and 206 lipid species were identified with their molecular structures in saliva, plasma, and fecal samples, respectively. Following identification, targeted quantification based on the selective reaction monitoring method was performed on individual samples. We excluded lipid species below the LOQ, and the number of quantified species was screened to 297, 202, and 166 in saliva, plasma, and fecal samples, respectively. The quantified results, including the average lipid concentrations for each group, are listed in Table S5, and the detailed molecular structures of the PC, PE, and TG species are listed in Table S6.

3.2. Alterations in lipid profiles of Saliva, plasma, and fecal samples in NSCLC patients

Figure 1 shows the PCA plots generated using all quantified lipid species, to visualize the changes in the lipid profiles of different sample types between LC and control groups. Each data point represented the overall lipid profile of an individual patient. The LC and control data points clustered apart from each other, with the differences being more prominent in the saliva and plasma samples than in the fecal samples, indicating distinct alterations in lipid profiles associated with the development of LC. The level of each lipid species in the LC and control groups was observed through volcano plots ($-\log_{10}$ (p value) vs. $\log_2$ (fold change)), as shown in Figure 2. In saliva samples, many lipids significantly decreased in concentration (upper left domain), while in plasma samples, a considerable number of lipids decreased significantly ($p < 0.01$), with less severe fold-changes compared with the salivary lipids. In fecal samples, only a few lipid species significantly increased in concentration (upper-right domain).

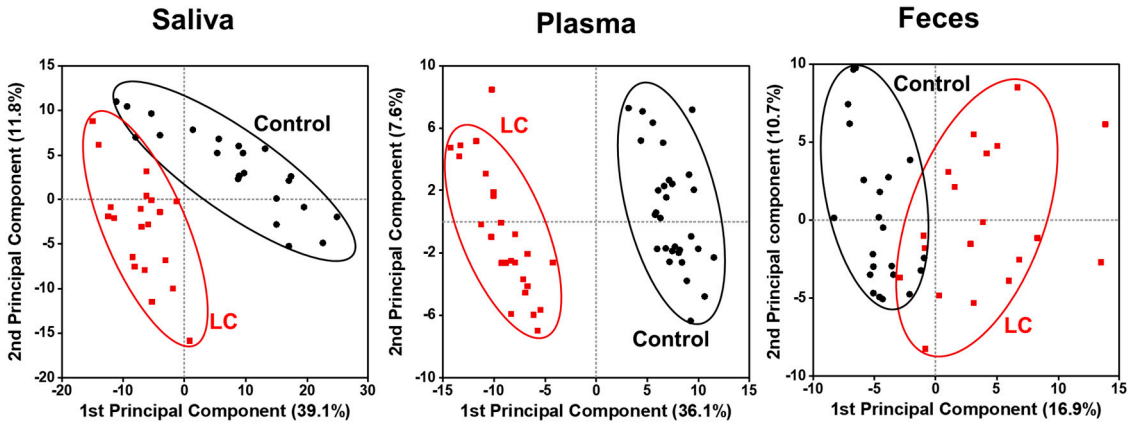

Figure 1. Principal component analysis (PCA) plots showing differences in lipid profiles of patients with lung cancer (LC) in comparison to controls in which all plots were based on all quantified lipid species.

Preprints (www.preprints.org) | NOT PEER-REVIEWED | Posted: 7 August 2023 doi:10.20944/preprints202308.0522.v1

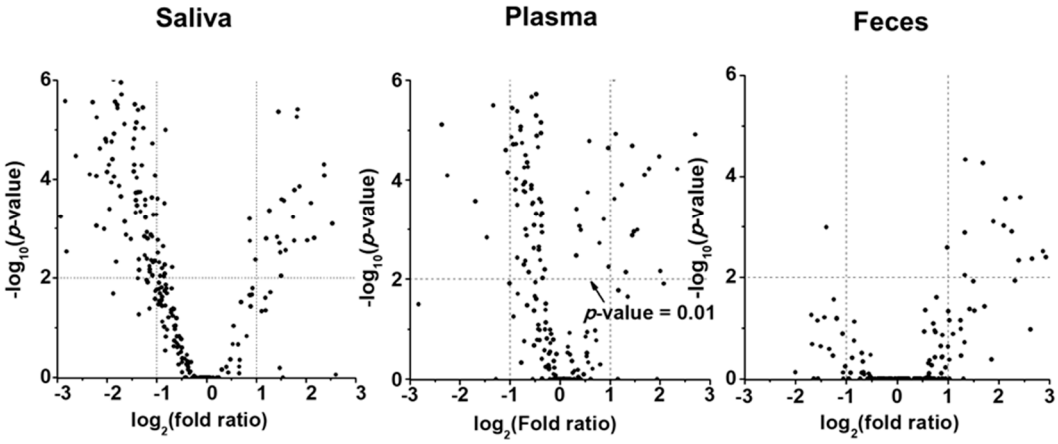

Figure 2. Volcano plots, *−log10(p-value) vs. log2(fold ratio),* of quantified lipid species showing the perturbation in lipid level based on statistical comparison. Fold ratio represents the ratio of a species' concentration of lung cancer (LC) to that of control.

The changes in lipid patterns in lipid categories, including glycerophospholipid (GP), sphingolipid (SP), glycerolipid (GL) comprising DG and TG, and CE, are depicted in Figure 3a. The stacked bar graphs showed the total concentrations of the four lipid classes, with the scale normalized to 100% for each control level (right axis). The total concentration of the four lipid classes increased in both saliva (approx. 47%) and fecal (approx. 62%) samples in the LC group compared with the control. The increase in fecal lipids of LC was primarily driven by an increase in SP (approx. 2.5 times), GL (approx. 40%), and CE (approx. 5.1 times). In contrast, GL in saliva increased approximately 2.5 times, while GP and SP in saliva decreased to approximately half of the levels seen in controls. A more detailed examination of the GP levels was conducted by comparing the total lipid levels of eight different classes of GPs (Figure 3b). Although PC, PE, and PI in fecal samples showed minimal changes, except for an increase in PG with LC, all GP classes in saliva samples exhibited a nearly two-fold decrease ($p < 0.01$). Notably, the number of PC and PE species identified in fecal samples was much lower than that in the saliva and plasma samples, and their total amounts were also considerably lower. Additionally, endogenous PS is typically not detected in the blood plasma or serum, but several PS species have been detected at substantial levels in the saliva. Furthermore, the levels of PC, PE, and PI in the saliva were much lower (a few to several 100-fold) than those in the plasma, whereas salivary PA levels were significantly higher.

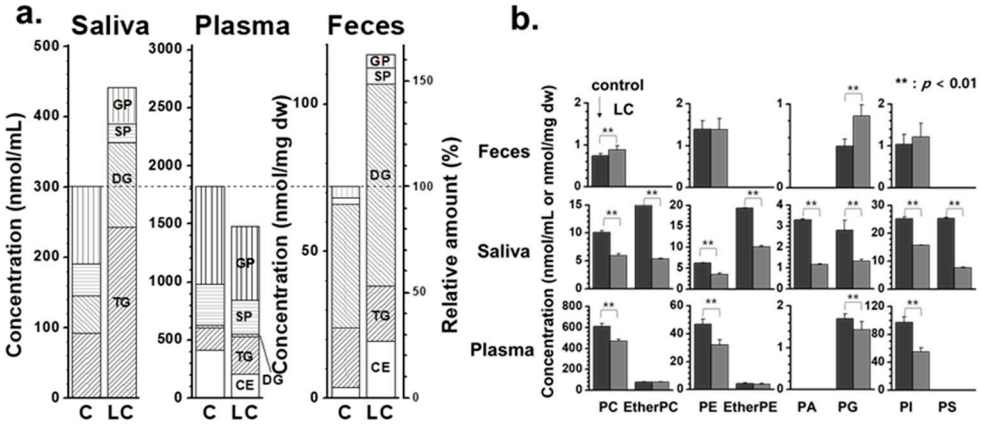

Figure 3. a) Stacked bar graphs showing the summed concentration level of four lipid classes (GP: glycerophospholipid, SP: sphingolipid, GL: glycerolipid, and CE: cholesteryl ester) of fecal, saliva, and plasma samples with lung cancer (LC) compared to controls. b) bar graphs showing the change in concentrations of each glycerophospholipid class.

Preprints (www.preprints.org) | NOT PEER-REVIEWED | Posted: 7 August 2023 doi:10.20944/preprints202308.0522.v1

A heat map of individual lipid species, selected based on their high abundance within each class and significant changes ($p < 0.01$) between the LC and control groups, provides a visual representation of the alterations, as shown in Figure 4. High abundance lipid species were defined as lipids with a relative abundance greater than 100% /n (n = number of lipids within each class). The saliva samples exhibited a significant decrease in the levels of selected GP and SP lipids, whereas most DG and TG species showed substantial increases. In plasma samples, GP, SP, and CE lipids decreased by approximately 17–50% in LC, whereas GL lipids increased by approximately 61%, resulting in an overall decrease (approx. 19%) in lipid levels. Salivary CE were not included in the heat map because of their low levels compared to plasma and fecal samples. However, a decrease in GP and SP lipids and an increase in GL lipids was observed in both the saliva and plasma samples.

To further understand the alterations in individual lipid levels, bar graphs were generated to show the fold ratios (LC/C) of the selected lipids (64, 36, and 28 species from the saliva, plasma, and fecal samples, respectively) that exhibited statistical differences ($p < 0.05$), as depicted in Figure S2 of the Supplementary Material. Among these, high-abundance lipid species showing fold ratios > 2.0 or < 0.5 were selected for further analysis, as shown in Figure 5. In saliva, selected GP and SP lipids were decreased by more than two-fold, whereas three DGs (32:0, 34:1, and 34:2) and six TGs (50:2, 52:2, 52:3, 52:5, 54:3, and 54:4) were significantly ($p < 0.05$) increased. In the plasma samples, only a few lipid species showed significant decreases (PI 38:4, three Cers (d40:1, d42:1, and d42:2), and CE 18:2), whereas five TGs (50:2, 52:4, 52:5, 54:4, and 54:6) were increased in the LC. In fecal samples, several ceramides (d34:0, d34:1, and d42:2), including two HexCers (d34:2 and d42:2) and two CEs (16:1 and 18:2), were increased more than 2-fold in LC.

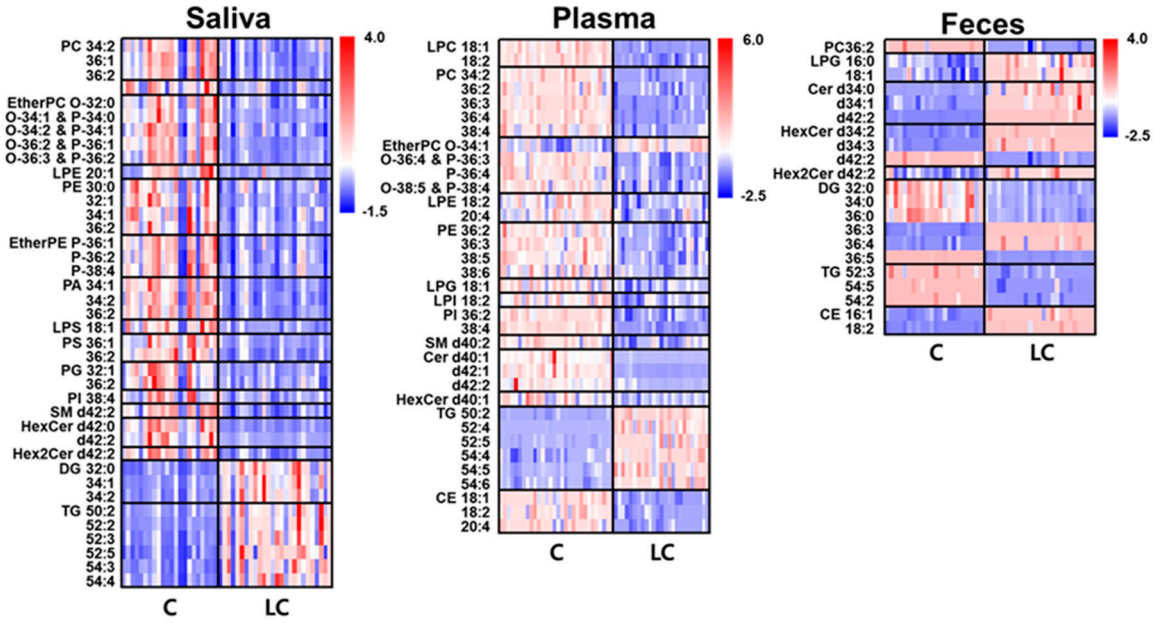

Figure 4. Heat map of high abundant lipid species showing significant differences ($p < 0.05$ by two-way ANOVA) in lipid levels.

Preprints (www.preprints.org) | NOT PEER-REVIEWED | Posted: 7 August 2023 doi:10.20944/preprints202308.0522.v1

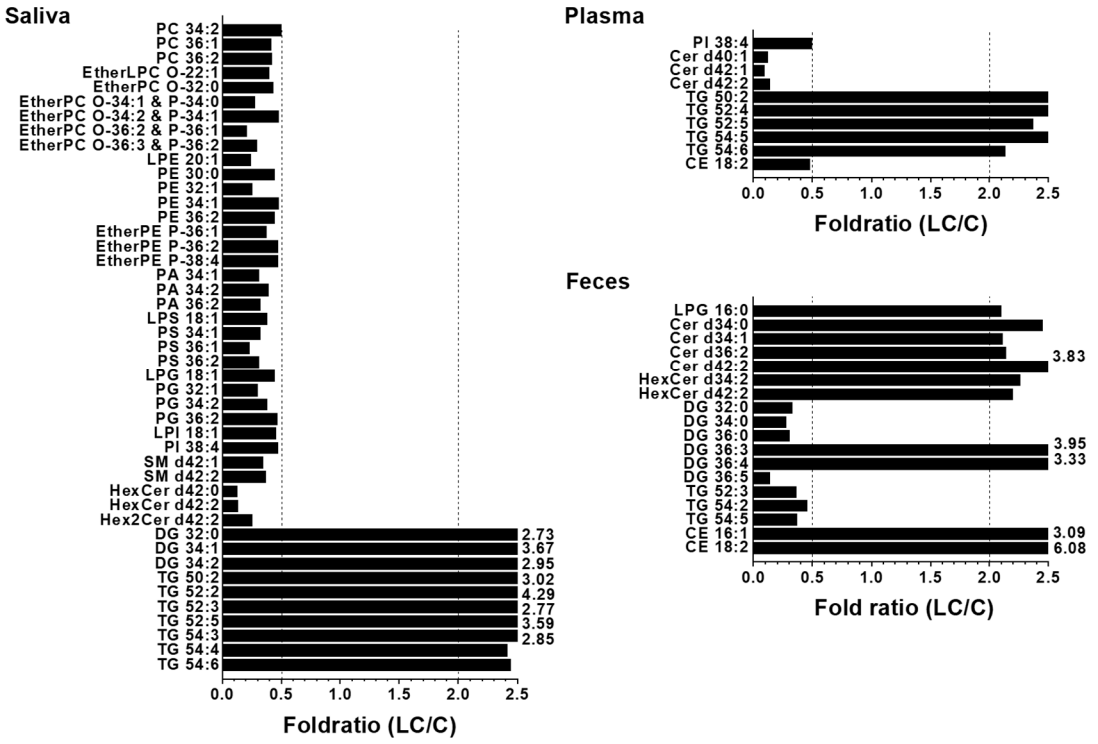

Figure 5. Bar graphs showing the fold ratio (LC/C) of lipid species matching with the criteria of high abundance species in each lipid class, > 2-fold change, and $p < 0.05$ in fecal, saliva, and plasma samples with LC compared to controls.

Additionally, three saturated DGs (32:0, 34:0, and 36:0) and three unsaturated TGs (52:3, 54:2, and 54:5) decreased by more than 2-fold, while two unsaturated DGs (36:3 and 36:4) increased by more than 3-fold in the LC. Among the lipids shown in Figure 5, those commonly found in at least two of the three sample types were selected and plotted in Figure 6. Notably, three TGs (50:2, 52:5, and 54:6) significantly increased (> 2-fold; $p < 0.05$) in all three sample types. Both Cer d42:2 and HexCer d42:2 levels were significantly increased in fecal samples but decreased in saliva samples, and DG 32:0 and TG 52:3 levels were decreased in fecal samples but increased in saliva samples. PI 38:4 exhibited a decrease of approximately 2-fold in both plasma and saliva.

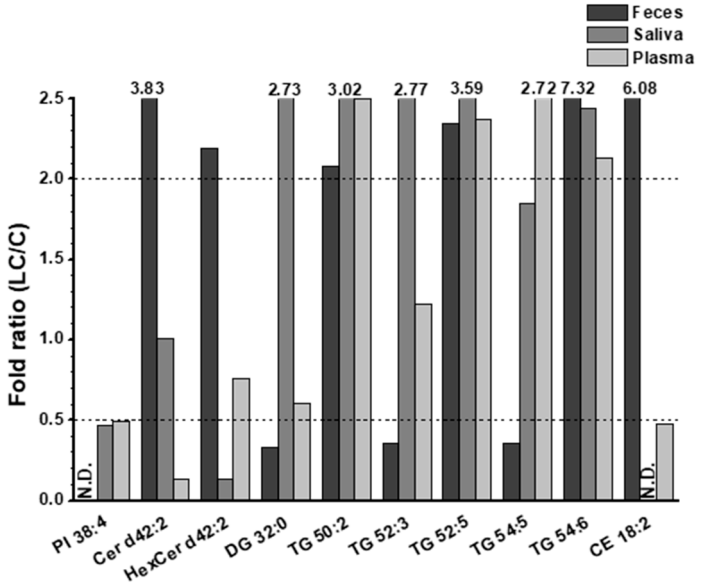

Figure 6. Selected lipid species commonly found in at least two types of samples in Figure 5.

Preprints (www.preprints.org) | NOT PEER-REVIEWED | Posted: 7 August 2023 doi:10.20944/preprints202308.0522.v1

Lipids that were significantly altered in the saliva, plasma, and feces were further examined by receiver operating characteristic (ROC) analysis to screen for species concerning LC; subsequently, the area under the curve (AUC) value of ROC analysis was calculated for each species. Table 1 lists the candidate lipid markers showing an AUC > 0.800, which were a) unique to each sample type and b) found in at least two sample types. Table 1 is limited to lipid species showing a > 2-fold change.

Table 1. List of candidate lipid molecules with significant changes (high abundance, > 2-fold change, and $p < 0.05$) with area under curve (AUC) value > 0.800 from receiver operating characteristic (ROC) analysis that were a) unique to each sample and b) common to two types of samples.

	Saliva				Plasma		Feces	
	Molecular species	AUC	Molecular species	AUC	Molecular species	AUC	Molecular species	AUC
a)	PC 36:1	0.840	PS 36:1	0.902	PI 38:4	1.000	LPG 16:0	0.846
	PC 36:2	0.831	PS 36:2	0.928	Cer d40:1	1.000	Cer d34:0	0.827
	EtherPC O-34:1 & P-34:0	0.885	PG 32:1	0.815	Cer d42:1	1.000	Cer d34:1	0.981
	EtherPC O-34:2 & P-34:1	0.817	SM d42:1	0.881	TG 50:2	1.000	Cer d34:2	0.875
	EtherPC O-36:2 & P-36:1	0.913	SM d42:2	0.837	TG 52:4	0.969	DG 32:0	0.967
	EtherPC O-36:3 & P-36:2	0.841	HexCer d42:0	0.940	TG 54:6	0.864	DG 34:0	0.978
	PE 32:1	0.866	HexCer d42:2	0.872			DG 36:0	0.971
	EtherPE P-36:1	0.835	Hex2Cer d42:2	0.861			DG 36:3	1.000
	PA 34:1	0.911	DG 32:0	0.928			DG 36:4	0.907
	PA 34:2	0.872	DG 34:1	0.872			DG 36:5	1.000
	PA 36:2	0.914	DG 34:2	0.810			TG 54:2	1.000
	LPS 18:1	0.815	TG 52:2	0.847			CE 16:1	0.950
	PS 34:1	0.936						
b)					Cer d42:2	0.948	Cer d42:2	1.000
			TG 52:3	0.806			TG 52:3	0.950
			TG 52:5	0.844	TG 52:5	0.927		
					TG 54:5	0.912	TG 54:5	1.000
					CE 18:2	0.930	CE 18:2	1.000

4. Discussion

LPC levels are clinical diagnostic indicators and important signaling molecules that regulate cell proliferation and inflammation. Previous studies have shown that the serum levels of LPC 18:1 and 18:2 decreased in patients with lung cancer [33,34]; this finding was consistent with the significant ($p < 0.05$) decrease observed in the plasma samples in this study. PC and PE are the most abundant glycerophospholipids in cell membranes, and the amounts of polyunsaturated PC and PE, as well as their ratios, are crucial for maintaining homeostasis [35]. In this study, most PC and PE species significantly decreased in both plasma and saliva samples (especially PC 34:2, PC 36:2, and PE 36:2 that were common to both sample types) in LC. These findings were similar to those of previous studies that analyzed plasma samples from both benign and malignant lung nodules [36] and observed significant decreases in most PE species in the plasma of patients with LC [37], as well as a decrease in PE 36:2 [9]. Moreover, most etherPC (or PC plasmalogen) and etherPE (or PE plasmalogen) species significantly decreased in saliva samples from patients with LC, whereas alterations were not as pronounced in the plasma samples (Table S5). Lung tissue is particularly susceptible to reactive oxygen species due to its direct exposure to oxygen, and ether lipids are known to play protective roles against oxidative stress. Therefore, a decrease in ether lipid levels can be attributed to increased oxidative stress during lung cancer development. In this study, ether lipid levels were significantly lower in saliva than in plasma. Previous studies analyzing malignant pleural effusion samples from patients with lung cancer revealed significant decreases in several etherPC

and etherPE species [38], and plasma lipid analysis showed a decrease in etherPE P-38:4 in lung cancer [9]. Among them, ether PC O-34:2 and three EtherPE species, P-36:1, P-36:2, and P-38:4, were significantly reduced in saliva samples. Because saliva has been used for miRNA analysis for the early detection of malignant pleural effusion caused by LC [39], a decrease in etherPE in the saliva can be a good indicator for the development of lung cancer.

PS plays a key role as a signaling molecule in the cell cycle related to apoptosis and is commonly found in the inner leaflets of cell membranes. Although PS is readily detected in mammalian cells, tissues, and urinary exosomes, endogenous PS molecules are rarely detected in human serum or plasma samples. In this study, PS species were not detected above the LOD in plasma and fecal samples. However, 11 of 18 PS species were significantly decreased (2–5 folds, $p < 0.01$) in saliva samples from patients with LC. These findings were similar to the significant decrease observed in several PS species obtained from malignant lung tissue of patients with NSCLC [10], and among these, PS 36:1 was found to constitute approximately 64% of all PS levels in our saliva samples and showed a significant decrease (fold ratio = 0.23 ± 0.03, $p < 0.01$). A previous study on the role of serine metabolism in LC suggested that the decrease in PS could be caused by the overexpression of SHMT 1/2, an enzyme responsible for converting serine to glycine and regulating cell growth in LC cells [40]. Therefore, the selective detection of PS 36:1 in saliva with a subsequent decrease could be a good alternative for diagnosing LC.

PG and PI, which play the role of pulmonary surfactants in the pulmonary alveoli of the lungs, are known to exert anti-inflammatory effects, and their levels in surfactant complexes are relatively higher (approx. > 100-fold) than in other tissues or mucosal surfaces [41]. Highly abundant PGs (32:1, 34:1, 34:2, and 36:2), which comprised approximately 68% of total PGs in saliva samples, were significantly reduced (2–3 folds, $p < 0.01$) in LC, although the levels of PGs in plasma with lung cancer were below the LOD in this study. The decreased PG levels in the saliva were consistent with the results of lipid analysis of the lung tissue of patients with LC [29], which exhibited significant decreases in PG 34:1 and 34:2. PI is a major contributor to arachidonic acid (AA, 20:4), a precursor of eicosanoids involved in inhibiting inflammation and the immune response [42]. A previous study showed that AA levels were significantly lower in the plasma of patients with LC, possibly leading to a reduction in the production of PI 38:4 [43]. In this study, PI 38:4 was found to significantly decrease (> 2 -folds, $p < 0.05$) in both the saliva and plasma of patients with LC, supporting its potential as a good candidate lipid for differentiating LC in the saliva and plasma.

Cer is involved in important cellular processes, such as the cell cycle, differentiation, aging, and apoptosis. Cer also serves as a central component of the metabolism of various sphingolipids. Cer is converted to SM through SM synthase, which transfers the phosphocholine moiety from PC to Cer, resulting in DG production. Conversely, SM can be converted back to Cer by sphingomyelinase (SMase). The accumulation of Cer in fluid samples of patients with LC can be explained by the conversion of SM to Cer via SMase [44]. In this study, it was observed that most SM levels in saliva decreased (> 2–3 folds, $p < 0.01$) with an increase in the two abundant Cer species (d34:0 and d34:1). However, the majority of SM species in the plasma did not show significant changes due to LC, although there were significant decreases in most Cer species. Determining the exact reason for fluctuations in Cer levels was challenging because the conversion between SM and Cer was not the sole pathway influencing the relative levels of these lipids and the level of SM was much higher than the total Cer level (5–10 times higher in our study). Nonetheless, it is known that a decrease in Cer levels could be associated with cancer cell resistance to apoptosis, and Cer species with acyl chains of C16, C18, and C24 have been found to be decreased in lung tumors and non-squamous head and neck cancers [45]. In this study, most Cer levels in the plasma (mainly d18:1/22:0, d18:1/24:0, and d18:1/24:1) were significantly decreased (> 7-folds, $p < 0.01$) in the presence of LC. However, the majority of Cer levels in the saliva remained unchanged, except for a decrease in Cer d18:1/24:0 (fold ratio = 0.58, $p < 0.05$). Interestingly, Cer levels increased by more than 2-folds in fecal samples ($p < 0.01$). While a previous study reported a decrease in the plasma levels of Cer d18:1/24:1 in LC [9], we noted that Cer d18:1/24:0 exhibited significant decreases in both plasma and saliva, but increased in fecal samples.

CE is a sterol formed when cholesterol is esterified with fatty acids, which results in its inactive form. Previous reports have indicated a significant accumulation of CE and cholesterol in human lung tumor tissues [46]. In a transgenic mouse model of KRAS-driven lung adenocarcinoma, increased activity of the Myc transcription factor that regulates cholesterol homeostasis and cell growth led to an imbalance between cholesterol influx and efflux in tumors and accumulation of CE in lipid droplets [47]. In our study, high-abundance CE species (18:1, 18:2, and 20:4, comprising approximately 85% of total CE) were significantly decreased (approximately 2-fold, $p < 0.01$) in plasma samples from individuals with LC, whereas 18:2 and 20:4 CE increased in fecal samples. Unfortunately, CE levels in saliva were not reported as they were below the LOQ. Notably, CE 18:2 levels are reported to decrease in the plasma of patients with squamous cell LC [48].

In cancer cells, fatty acid (FA) synthesis is often accelerated because of the reprogramming of FA metabolism, and the accumulated FAs are stored in the form of triglycerides (TG) [49]. Several studies have reported increased levels of TG in LC tissues, which are attributed to the overexpression of enzymes (ACLY and ACC) that promote FA synthesis and contribute to the progression of NSCLC [49]. In our study, TG levels were found to be significantly increased (more than 2–3-fold) in both plasma and saliva samples from individuals with LC but decreased in fecal samples. Among them, TG 54:4 showed significant increases (fold ratio = 3.90 ± 0.19, $p < 0.05$) in plasma with lung cancer [9], and it was also commonly increased in both saliva (fold ratio = 2.41 ± 0.40, $p < 0.01$) and plasma (fold ratio = 1.84 ± 0.89, $p < 0.01$) samples in our study. However, it is noted that three TGs (50:2, 52:5, and 54:6) were significantly increased in all sample types. DG is a metabolic intermediate of TG that plays a crucial role in the synthesis of glycerophospholipids in cell membranes. The levels of most DGs significantly increased in the saliva, whereas their alterations in plasma were minimal at relatively low levels. In fecal samples, saturated DGs (32:0, 34:0, and 36:0) decreased by more than 3-fold, whereas unsaturated DGs (36:2, 36:3, and 36:4) increased by more than 2–3-fold.

Comparison of the saliva, plasma, and feces lipid profiles with LC showed that the lipid distribution in fecal samples did not show a strong correlation with that in plasma and saliva samples. However, there was some similarity between plasma and saliva samples. The overall levels of glycerophospholipids and sphingolipids in the fecal samples were relatively low and not informative for assessing changes related to LC. In contrast, significant changes were observed in neutral lipids, particularly DG. Using ROC analysis, we identified 27, 16, and 10 lipid molecules as potential biomarkers specific to the saliva, feces, and plasma samples, respectively, of patients with LC. Among these molecules, three species (Cer d42:2, TG 54:5, and CE 18:2) were common to both feces and plasma samples, two species (DG 32:0 and TG 52:3) were common to both feces and saliva samples, and only one species (TG 52:5) was common to saliva and plasma samples.

Although saliva and plasma samples exhibited similar patterns of lipid class level changes, the degree of change in each lipid class or individual lipid level in plasma samples was less severe than that in saliva samples. This was reflected in the smaller number of significantly altered lipids in plasma than in saliva. Despite the lower total lipid level in saliva (approximately six times less than that in plasma), the changes in salivary lipid levels were more distinct than those in plasma lipids in our study. This suggested that alterations in salivary lipid distribution could provide more information about cellular lipid metabolism, which could better reflect physiological states than circulating blood that is diluted throughout the body.

Supplementary Materials: The following supporting information can be downloaded at the website of this paper posted on Preprints.org, Figure S1: Base peak chromatograms of lipid extracts from saliva, plasma, and feces of patients with NSCLC at positive (ESI+) and negative (ESI-) ion modes of nUHPLC-ESI-MS/MS; Figure S2: Bar graphs showing fold ratio (LC/C) of each lipid species with statistical significance ($p < 0.05$) in fecal, saliva, and plasma samples with LC compared to controls; Table S1: List of lipid standards used for this study. Lipids marked with * were used to prepare an internal standard lipid mixture; Table S2: Type of precursor and quantifier ions of each lipid class and collision energy for SRM quantification; Table S3: Slopes and intercepts of the calibration curve of each lipid class; Table S4: Limit of detection (LOD) and limit of quantitation (LOQ) values of external lipid standards based on calibration curves and the type of internal standards spiked to lipid extracts by nUHPLC-ESI-MS/MS; Table S5: Concentration of lipid species (nmol/mL) in saliva, plasma, and fecal samples from both the control and the lung cancer groups. Lipid concentration was calculated from a calibration curve

of each lipid class. Species marked with underline for high abundance species in each lipid class. Numbers in the parenthesis represent the quantified/identified numbers of lipids. N.D. represents for "not detectable" as below LOD (S/N = 3). Concentration values marked with grey represent for the calculated concentration below LOQ (S/N=10). Lipid concentration was calculated from a calibration curve of each lipid class. Species marked with underline for high abundance species in each lipid class. Numbers in the parenthesis represent the quantified/identified numbers of lipids. N.D. represents for "not detectable" as below LOD (S/N = 3). Concentration values marked with grey represent for the calculated concentration below LOQ (S/N=10); Table S6: Isomeric structure of PC, PE, and TG identified from CID spectra.

Author Contributions: B.Y. Hwang and J.W. Seo carried out the lipidomic analysis and data curation. C.Muftuoglu, U. Mert, and M. Asadi performed on conceptualization and investigation. F. Guldaval, H.S. Karakus, T. Goksel, and A. Veral were for patient follow-up, A. Caner conceptualized experiments, wrote and edited original draft. M.H. Moon supervised lipidomic analysis, wrote and edited the manuscript. All the authors discussed and approved the final manuscript.

Funding: This work was supported by the bilateral research program (NRF-2020K2A9A1A06097918 and TUBITAK-120N924) between Turkey and Korea, the National Research Foundation (NRF) of Korea, and in part by NRF-2021R1A2C2003171.

Institutional Review Board Statement: The study was conducted in accordance with the Declaration of Helsinki, and approved by the Ethics Committee of Ege University (19-9T/66 and 09.09.2019) and lipidomic analysis was approved by the Institutional Review Board of Yonsei University (IRB No. 7001988-202105-BR-1215-03).

Informed Consent Statement: Informed consent was obtained from all subjects involved in the study.

Conflicts of Interest: There are no conflict of interest to declare.

References

1. Bray, F.; Ferlay, J.; Soerjomataram, I.; Siegel, R.L.; Torre, L.A.; Jemal, A. Global cancer statistics 2018: GLOBOCAN estimates of incidence and mortality worldwide for 36 cancers in 185 countries. *CA: A Cancer Journal for Clinicians* **2018**, *68*, 394-424, doi:https://doi.org/10.3322/caac.21492.
2. Thai, A.A.; Solomon, B.J.; Sequist, L.V.; Gainor, J.F.; Heist, R.S. Lung cancer. *The Lancet* **2021**, *398*, 535-554, doi:https://doi.org/10.1016/S0140-6736(21)00312-3.
3. Knight, S.B.; Crosbie, P.A.; Balata, H.; Chudziak, J.; Hussell, T.; Dive, C. Progress and prospects of early detection in lung cancer. *Open Biol* **2017**, *7*, doi:ARTN 170070, 10.1098/rsob.170070.
4. Holčapek, M.; Liebisch, G.; Ekroos, K. Lipidomic Analysis. *Analytical Chemistry* **2018**, *90*, 4249-4257, doi:10.1021/acs.analchem.7b05395.
5. Knittelfelder, O.L.; Weberhofer, B.P.; Eichmann, T.O.; Kohlwein, S.D.; Rechberger, G.N. A versatile ultra-high performance LC-MS method for lipid profiling. *Journal of Chromatography B* **2014**, *951-952*, 119-128, doi:https://doi.org/10.1016/j.jchromb.2014.01.011.
6. García-Cañaveras, J.C.; Donato, M.T.; Castell, J.V.; Lahoz, A. A Comprehensive Untargeted Metabonomic Analysis of Human Steatotic Liver Tissue by RP and HILIC Chromatography Coupled to Mass Spectrometry Reveals Important Metabolic Alterations. *Journal of Proteome Research* **2011**, *10*, 4825-4834, doi:10.1021/pr200629p.
7. Zhao, Y.Y.; Miao, H.; Cheng, X.L.; Wei, F. Lipidomics: Novel insight into the biochemical mechanism of lipid metabolism and dysregulation-associated disease. *Chem Biol Interact* **2015**, *240*, 220-238, doi:10.1016/j.cbi.2015.09.005.
8. Santos, C.R.; Schulze, A. Lipid metabolism in cancer. *FEBS J* **2012**, *279*, 2610-2623, doi:10.1111/j.1742-4658.2012.08644.x.
9. Lee, G.B.; Lee, J.C.; Moon, M.H. Plasma lipid profile comparison of five different cancers by nanoflow ultrahigh performance liquid chromatography-tandem mass spectrometry. *Analytica Chimica Acta* **2019**, *1063*, 117-126, doi:https://doi.org/10.1016/j.aca.2019.02.021.
10. Marien, E.; Meister, M.; Muley, T.; Fieuws, S.; Bordel, S.; Derua, R.; Spraggins, J.; Van de Plas, R.; Dehairs, J.; Wouters, J.; et al. Non-small cell lung cancer is characterized by dramatic changes in phospholipid profiles. *Int J Cancer* **2015**, *137*, 1539-1548, doi:10.1002/ijc.29517.
11. Noreldeen, H.A.A.; Du, L.; Li, W.; Liu, X.; Wang, Y.; Xu, G. Serum lipidomic biomarkers for non-small cell lung cancer in nonsmoking female patients. *J Pharm Biomed Anal* **2020**, *185*, 113220, doi:10.1016/j.jpba.2020.113220.
12. Siqueira, W.L.; Zhang, W.; Helmerhorst, E.J.; Gygi, S.P.; Oppenheim, F.G. Identification of Protein Components in in vivo Human Acquired Enamel Pellicle Using LC−ESI−MS/MS. *Journal of Proteome Research* **2007**, *6*, 2152-2160, doi:10.1021/pr060580k.

13. Freitas, D.; Le Feunteun, S. Oro-gastro-intestinal digestion of starch in white bread, wheat-based and gluten-free pasta: Unveiling the contribution of human salivary α-amylase. *Food Chemistry* **2019**, *274*, 566-573, doi:https://doi.org/10.1016/j.foodchem.2018.09.025.
14. Agatonovic-Kustrin, S.; Morton, D.W.; Smirnov, V.; Petukhov, A.; Gegechkori, V.; Kuzina, V.; Gorpinchenko, N.; Ramenskaya, G. Analytical Strategies in Lipidomics for Discovery of Functional Biomarkers from Human Saliva. *Dis Markers* **2019**, *2019*, 6741518, doi:10.1155/2019/6741518.
15. Turunen, S.; Puurunen, J.; Auriola, S.; Kullaa, A.M.; Kärkkäinen, O.; Lohi, H.; Hanhineva, K. Metabolome of canine and human saliva: a non-targeted metabolomics study. *Metabolomics* **2020**, *16*, 90, doi:10.1007/s11306-020-01711-0.
16. de Oliveira, L.R.P.; Martins, C.; Fidalgo, T.K.S.; Freitas-Fernandes, L.B.; de Oliveira Torres, R.; Soares, A.L.; Almeida, F.C.L.; Valente, A.P.; de Souza, I.P.R. Salivary Metabolite Fingerprint of Type 1 Diabetes in Young Children. *Journal of Proteome Research* **2016**, *15*, 2491-2499, doi:10.1021/acs.jproteome.6b00007.
17. Sun, Y.; Liu, S.; Qiao, Z.; Shang, Z.; Xia, Z.; Niu, X.; Qian, L.; Zhang, Y.; Fan, L.; Cao, C.-X.; et al. Systematic comparison of exosomal proteomes from human saliva and serum for the detection of lung cancer. *Analytica Chimica Acta* **2017**, *982*, 84-95, doi:https://doi.org/10.1016/j.aca.2017.06.005.
18. Lee, G.B.; Caner, A.; Moon, M.H. Optimisation of saliva volumes for lipidomic analysis by nanoflow ultrahigh performance liquid chromatography-tandem mass spectrometry. *Analytica Chimica Acta* **2022**, *1193*, 339318, doi:https://doi.org/10.1016/j.aca.2021.339318.
19. Karu, N.; Deng, L.; Slae, M.; Guo, A.C.; Sajed, T.; Huynh, H.; Wine, E.; Wishart, D.S. A review on human fecal metabolomics: Methods, applications and the human fecal metabolome database. *Analytica Chimica Acta* **2018**, *1030*, 1-24, doi:https://doi.org/10.1016/j.aca.2018.05.031.
20. Raman, M.; Ahmed, I.; Gillevet, P.M.; Probert, C.S.; Ratcliffe, N.M.; Smith, S.; Greenwood, R.; Sikaroodi, M.; Lam, V.; Crotty, P.; et al. Fecal Microbiome and Volatile Organic Compound Metabolome in Obese Humans With Nonalcoholic Fatty Liver Disease. *Clinical Gastroenterology and Hepatology* **2013**, *11*, 868-875.e863, doi:https://doi.org/10.1016/j.cgh.2013.02.015.
21. Jia, P.; Wang, S.; Xiao, C.; Yang, L.; Chen, Y.; Jiang, W.; Zheng, X.; Zhao, G.; Zang, W.; Zheng, X. The anti-atherosclerotic effect of tanshinol borneol ester using fecal metabolomics based on liquid chromatography-mass spectrometry. *Analyst* **2016**, *141*, 1112-1120, doi:10.1039/C5AN01970B.
22. Bjerrum, J.T.; Wang, Y.; Hao, F.; Coskun, M.; Ludwig, C.; Günther, U.; Nielsen, O.H. Metabonomics of human fecal extracts characterize ulcerative colitis, Crohn's disease and healthy individuals. *Metabolomics* **2015**, *11*, 122-133, doi:10.1007/s11306-014-0677-3.
23. Gregory, K.E.; Bird, S.S.; Gross, V.S.; Marur, V.R.; Lazarev, A.V.; Walker, W.A.; Kristal, B.S. Method Development for Fecal Lipidomics Profiling. *Analytical Chemistry* **2013**, *85*, 1114-1123, doi:10.1021/ac303011k.
24. Van Meulebroek, L.; De Paepe, E.; Vercruysse, V.; Pomian, B.; Bos, S.; Lapauw, B.; Vanhaecke, L. Holistic Lipidomics of the Human Gut Phenotype Using Validated Ultra-High-Performance Liquid Chromatography Coupled to Hybrid Orbitrap Mass Spectrometry. *Anal Chem* **2017**, *89*, 12502-12510, doi:10.1021/acs.analchem.7b03606.
25. Ertl, V.M.; Horing, M.; Schott, H.F.; Blucher, C.; Kjolbaek, L.; Astrup, A.; Burkhardt, R.; Liebisch, G. Quantification of diacylglycerol and triacylglycerol species in human fecal samples by flow injection Fourier transform mass spectrometry. *Anal Bioanal Chem* **2020**, *412*, 2315-2326, doi:10.1007/s00216-020-02416-y.
26. Coleman, M.J.; Espino, L.M.; Lebensohn, H.; Zimkute, M.V.; Yaghooti, N.; Ling, C.L.; Gross, J.M.; Listwan, N.; Cano, S.; Garcia, V.; et al. Individuals with Metabolic Syndrome Show Altered Fecal Lipidomic Profiles with No Signs of Intestinal Inflammation or Increased Intestinal Permeability. *Metabolites* **2022**, *12*, doi:10.3390/metabo12050431.
27. Gao, B.; Zeng, S.; Maccioni, L.; Shi, X.; Armando, A.; Quehenberger, O.; Zhang, X.; Starkel, P.; Schnabl, B. Lipidomics for the Prediction of Progressive Liver Disease in Patients with Alcohol Use Disorder. *Metabolites* **2022**, *12*, doi:10.3390/metabo12050433.
28. Cífková, E.; Brumarová, R.; Ovčačíková, M.; Dobešová, D.; Mičová, K.; Kvasnička, A.; Vaňková, Z.; Šiller, J.; Sákra, L.; Friedecký, D.; et al. Lipidomic and metabolomic analysis reveals changes in biochemical pathways for non-small cell lung cancer tissues. *Biochimica et Biophysica Acta (BBA) - Molecular and Cell Biology of Lipids* **2022**, *1867*, 159082, doi:https://doi.org/10.1016/j.bbalip.2021.159082.
29. Eggers, L.F.; Müller, J.; Marella, C.; Scholz, V.; Watz, H.; Kugler, C.; Rabe, K.F.; Goldmann, T.; Schwudke, D. Lipidomes of lung cancer and tumour-free lung tissues reveal distinct molecular signatures for cancer differentiation, age, inflammation, and pulmonary emphysema. *Scientific Reports* **2017**, *7*, 11087, doi:10.1038/s41598-017-11339-1.
30. Fan, Y.; Noreldeen, H.A.A.; You, L.; Liu, X.; Pan, X.; Hou, Z.; Li, Q.; Li, X.; Xu, G. Lipid alterations and subtyping maker discovery of lung cancer based on nontargeted tissue lipidomics using liquid chromatography-mass spectrometry. *J Pharm Biomed Anal* **2020**, *190*, 113520, doi:10.1016/j.jpba.2020.113520.

31. Cesbron, N.; Royer, A.L.; Guitton, Y.; Sydor, A.; Le Bizec, B.; Dervilly-Pinel, G. Optimization of fecal sample preparation for untargeted LC-HRMS based metabolomics. *Metabolomics* **2017**, *13*, 99, doi:10.1007/s11306-017-1233-8.
32. Koelmel, J.P.; Kroeger, N.M.; Ulmer, C.Z.; Bowden, J.A.; Patterson, R.E.; Cochran, J.A.; Beecher, C.W.W.; Garrett, T.J.; Yost, R.A. LipidMatch: an automated workflow for rule-based lipid identification using untargeted high-resolution tandem mass spectrometry data. *BMC Bioinformatics* **2017**, *18*, 331, doi:10.1186/s12859-017-1744-3.
33. Ros-Mazurczyk, M.; Jelonek, K.; Marczyk, M.; Binczyk, F.; Pietrowska, M.; Polanska, J.; Dziadziuszko, R.; Jassem, J.; Rzyman, W.; Widlak, P. Serum lipid profile discriminates patients with early lung cancer from healthy controls. *Lung Cancer* **2017**, *112*, 69-74, doi:10.1016/j.lungcan.2017.07.036.
34. Zhang, Q.; Xu, H.; Liu, R.; Gao, P.; Yang, X.; Jin, W.; Zhang, Y.; Bi, K.; Li, Q. A Novel Strategy for Targeted Lipidomics Based on LC-Tandem-MS Parameters Prediction, Quantification, and Multiple Statistical Data Mining: Evaluation of Lysophosphatidylcholines as Potential Cancer Biomarkers. *Anal Chem* **2019**, *91*, 3389-3396, doi:10.1021/acs.analchem.8b04715.
35. van der Veen, J.N.; Kennelly, J.P.; Wan, S.; Vance, J.E.; Vance, D.E.; Jacobs, R.L. The critical role of phosphatidylcholine and phosphatidylethanolamine metabolism in health and disease. *Biochim Biophys Acta Biomembr* **2017**, *1859*, 1558-1572, doi:10.1016/j.bbamem.2017.04.006.
36. Gao, L.; Wen, Z.; Wu, C.; Wen, T.; Ong, C.N. Metabolic profiling of plasma from benign and malignant pulmonary nodules patients using mass spectrometry-based metabolomics. *Metabolites* **2013**, *3*, 539-551, doi:10.3390/metabo3030539.
37. Lee, G.B.; Lee, J.C.; Moon, M.H. Plasma lipid profile comparison of five different cancers by nanoflow ultrahigh performance liquid chromatography-tandem mass spectrometry. *Anal Chim Acta* **2019**, *1063*, 117-126, doi:10.1016/j.aca.2019.02.021.
38. Yang, Z.; Song, Z.; Chen, Z.; Guo, Z.; Jin, H.; Ding, C.; Hong, Y.; Cai, Z. Metabolic and lipidomic characterization of malignant pleural effusion in human lung cancer. *J Pharm Biomed Anal* **2020**, *180*, 113069, doi:10.1016/j.jpba.2019.113069.
39. Yang, Y.; Ma, L.; Qiao, X.; Zhang, X.; Dong, S.F.; Wu, M.T.; Zhai, K.; Shi, H.Z. Salivary microRNAs show potential as biomarkers for early diagnosis of malignant pleural effusion. *Transl Lung Cancer Res* **2020**, *9*, 1247-1257, doi:10.21037/tlcr-19-530.
40. Zhou, X.; Tian, C.; Cao, Y.; Zhao, M.; Wang, K. The role of serine metabolism in lung cancer: From oncogenesis to tumor treatment. *Front Genet* **2022**, *13*, 1084609, doi:10.3389/fgene.2022.1084609.
41. Numata, M.; Voelker, D.R. Anti-inflammatory and anti-viral actions of anionic pulmonary surfactant phospholipids. *Biochim Biophys Acta Mol Cell Biol Lipids* **2022**, *1867*, 159139, doi:10.1016/j.bbalip.2022.159139.
42. van Dieren, J.M.; Simons-Oosterhuis, Y.; Raatgeep, H.C.; Lindenbergh-Kortleve, D.J.; Lambers, M.E.; van der Woude, C.J.; Kuipers, E.J.; Snoek, G.T.; Potman, R.; Hammad, H.; et al. Anti-inflammatory actions of phosphatidylinositol. *Eur J Immunol* **2011**, *41*, 1047-1057, doi:10.1002/eji.201040899.
43. Zhang, Y.; He, C.; Qiu, L.; Wang, Y.; Zhang, L.; Qin, X.; Liu, Y.; Zhang, D.; Li, Z. Serum unsaturated free Fatty acids: potential biomarkers for early detection and disease progression monitoring of non-small cell lung cancer. *J Cancer* **2014**, *5*, 706-714, doi:10.7150/jca.9787.
44. Piccinini, M.; Scandroglio, F.; Prioni, S.; Buccinna, B.; Loberto, N.; Aureli, M.; Chigorno, V.; Lupino, E.; DeMarco, G.; Lomartire, A.; et al. Deregulated sphingolipid metabolism and membrane organization in neurodegenerative disorders. *Mol Neurobiol* **2010**, *41*, 314-340, doi:10.1007/s12035-009-8096-6.
45. Ogretmen, B.; Hannun, Y.A. Biologically active sphingolipids in cancer pathogenesis and treatment. *Nat Rev Cancer* **2004**, *4*, 604-616, doi:10.1038/nrc1411.
46. Hoppstadter, J.; Dembek, A.; Horing, M.; Schymik, H.S.; Dahlem, C.; Sultan, A.; Wirth, N.; Al-Fityan, S.; Diesel, B.; Gasparoni, G.; et al. Dysregulation of cholesterol homeostasis in human lung cancer tissue and tumour-associated macrophages. *EBioMedicine* **2021**, *72*, 103578, doi:10.1016/j.ebiom.2021.103578.
47. Hall, Z.; Wilson, C.H.; Burkhart, D.L.; Ashmore, T.; Evan, G.I.; Griffin, J.L. Myc linked to dysregulation of cholesterol transport and storage in nonsmall cell lung cancer. *J Lipid Res* **2020**, *61*, 1390-1399, doi:10.1194/jlr.RA120000899.
48. Yu, Z.; Chen, H.; Zhu, Y.; Ai, J.; Li, Y.; Gu, W.; Borgia, J.A.; Zhang, J.; Jiang, B.; Chen, W.; et al. Global lipidomics reveals two plasma lipids as novel biomarkers for the detection of squamous cell lung cancer: A pilot study. *Oncol Lett* **2018**, *16*, 761-768, doi:10.3892/ol.2018.8740.
49. Eltayeb, K.; La Monica, S.; Tiseo, M.; Alfieri, R.; Fumarola, C. Reprogramming of Lipid Metabolism in Lung Cancer: An Overview with Focus on EGFR-Mutated Non-Small Cell Lung Cancer. *Cells* **2022**, *11*, doi:10.3390/cells11030413.